

# Energy levels, radiative rates and electron impact excitation rates for transitions in Al X<sup>\*</sup>

Kanti M. Aggarwal<sup>1</sup>† and Francis P. Keenan<sup>1</sup>

<sup>1</sup>*Astrophysics Research Centre, School of Mathematics and Physics, Queen's University Belfast, Belfast BT7 1NN, Northern Ireland, UK*

Accepted 2013 November 21. Received 2013 November 14; in original form 2013 August 1

## ABSTRACT

Energy levels, radiative rates and lifetimes are calculated among the lowest 98 levels of the  $n \leq 4$  configurations of Be-like Al X. The GRASP (General-purpose Relativistic Atomic Structure Package) is adopted and data are provided for all E1, E2, M1 and M2 transitions. Similar data are also obtained with the Flexible Atomic Code (FAC) to assess the accuracy of the calculations. Based on comparisons between calculations with the two codes as well as with available measurements, our listed energy levels are assessed to be accurate to better than 0.3%. However, the accuracy for radiative rates and lifetimes is estimated to be about 20%. Collision strengths are also calculated for which the Dirac Atomic R-matrix Code (DARC) is used. A wide energy range (up to 380 Ryd) is considered and resonances resolved in a fine energy mesh in the thresholds region. The collision strengths are subsequently averaged over a Maxwellian velocity distribution to determine effective collision strengths up to a temperature of  $1.6 \times 10^7$  K. Our results are compared with the previous (limited) atomic data and significant differences (up to a factor of 4) are noted for several transitions, particularly those which are not allowed in  $jj$  coupling.

**Key words:** atomic data – atomic processes

## 1 INTRODUCTION

Emission lines of Al ions are widely detected in a variety of plasmas, including solar and laser plasmas – see for example, Landi et al. (2001) and Gu, Beiersdorfer & Lepson (2011). Their observation provides diagnostics for which atomic data are required for a range of parameters, such as energy levels, radiative rates ( $A$ -values), and excitation rates or equivalently the effective collision strengths ( $\Upsilon$ ), which are obtained from the electron impact collision strengths ( $\Omega$ ). Emission lines of many Al ions are included in the CHIANTI database at <http://www.chiantidatabase.org/>, and for Al X are listed in the 35–60,600 Å wavelength range in the *Atomic Line List* (v2.04) of Peter van Hoof at <http://www.pa.uky.edu/~peter/atomic/>. Of particular interest are two transitions, namely  $2s^2 \ ^1S_0$ – $2s2p \ ^3P_1^o$  and  $2s2p \ ^3P_1^o$ – $2p^2 \ ^1D_2$ , at wavelengths of  $\sim 637$  and  $670$  Å, respectively. These have been measured in solar spectra from the Solar Ultraviolet Measurement of Emitted Radiation (SUMER) instrument on board the Solar and Heliospheric Observatory (SOHO). The ratio of their intensities is tem-

perature sensitive (Landi et al. 2001) and hence provides an excellent diagnostic. Since these lines are close in wavelength, they are readily detected by a single spectrograph, thus providing an additional advantage of accuracy.

Unfortunately, existing atomic data for Al X are very limited, particularly for collision strengths ( $\Omega$ ) and effective collision strengths ( $\Upsilon$ ). Zhang & Sampson (1992) calculated  $\Omega$  for 45 transitions among the lowest 10 levels of Be-like ions with  $8 \leq Z \leq 92$ , but did not report results for Al X. The only data available for  $\Upsilon$  are those of Keenan et al. (1986), who provided analytical expressions to derive interpolated values of  $\Upsilon$  based on  $R$ -matrix calculations for Be-like ions between C III and Si XI. Their results are only for transitions among the lowest 10 levels of the  $n=2$  configurations, and are incorporated in the CHIANTI database. No calculation has to our knowledge been performed with the  $R$ -matrix code which explicitly includes the contribution of resonances to the determination of  $\Upsilon$ . This may be highly significant, particularly for the forbidden transitions, as noted earlier for another Be-like ion, i.e. Ti XIX (Aggarwal & Keenan 2012c).

To analyse solar observations, Landi et al. (2001) adopted the atomic data for Al X in CHIANTI. Since these data are limited to transitions within the  $n=2$  configurations, they also calculated  $\Upsilon$  for a larger model, i.e. 98 levels of the  $n \leq 4$  configurations. For this they adopted the

\* Tables 2 and 5 are available only in the electronic version.

† E-mail: K.Aggarwal@qub.ac.uk(KMA); F.Keenan@qub.ac.uk (FPK)

Hebrew University Lawrence Livermore Atomic Code (HULLAC) of Bar-Shalom, Klapisch & Oreg (2001), based on the well-known and widely-used *distorted-wave* (DW) method. Since resonance contributions are not normally included in DW calculations, the results for  $\Upsilon$  may be significantly underestimated. Therefore, they included their contribution using the isolated resonance approximation. As a consequence, temperatures deduced from solar observations using two different sets of atomic data are significantly different, i.e.  $10^{6.47}$  and  $10^{5.75}$  K from CHIANTI and HULLAC, respectively.

The isolated resonance approximation takes into account the resonance contribution to a large extent, but  $\Upsilon$  can still be greatly underestimated, as demonstrated by Aggarwal & Keenan (2004, 2013) for transitions in Mo XXXIV and Fe XXV, respectively. Furthermore, Landi et al. (2001) did not list any atomic data and these are not available on any website. Therefore, in this work we report atomic data for energy levels, A- values,  $\Omega$  and  $\Upsilon$  for all transitions among the lowest 98 levels of the  $n \leq 4$  configurations of Al X. To determine the atomic structure (i.e. calculate energy levels and A- values) we employ the fully relativistic GRASP (General-purpose Relativistic Atomic Structure Package) code. Our version was originally developed by Grant et al. (1980) and is referred to as GRASP0, but has been significantly revised by one of its authors (Dr. P. H. Norrington), and is available at the website <http://web.am.qub.ac.uk/DARC/>. It is a fully relativistic code, based on the *jj* coupling scheme, and includes higher-order relativistic corrections arising from the Breit (magnetic) interaction and quantum electrodynamics (QED) effects (vacuum polarisation and Lamb shift). Furthermore, as in our earlier work, we have used the option of *extended average level* (EAL). Under this option a weighted (proportional to  $2j+1$ ) trace of the Hamiltonian matrix is minimised. However, the results obtained for energy levels as well as radiative rates are comparable to other options, such as *average level* (AL), as noted by Aggarwal, Keenan & Lawson (2008, 2010) for Kr and Xe ions.

For the scattering calculations, we have adopted the *Dirac Atomic R-matrix Code* (DARC) of P. H. Norrington and I. P. Grant (<http://web.am.qub.ac.uk/DARC/>). This is a relativistic version of the standard *R-matrix* code and is based on the *jj* coupling scheme. For this reason, the accuracy of calculated data (for  $\Omega$  and subsequently  $\Upsilon$ ) should be higher, particularly for transitions among the *fine-structure* levels of a state, because resonances through the energies of degenerating levels are also taken into account.

## 2 ENERGY LEVELS

The lowest 98 levels of Al X belong to the 17 configurations:  $(1s^2) 2l2l'$ ,  $2l3l'$  and  $2l4l'$ . Our level energies calculated from GRASP, *without* and *with* the inclusion of Breit and QED effects, are listed in Table 1. Martin & Zalubas (1979) have compiled and critically evaluated experimentally-measured energy levels of Al X, which are available at the NIST (National Institute of Standards and Technology) website <http://www.nist.gov/pml/data/asd.cfm>, and included in Table 1 for comparison. However, NIST energies are not available for many levels, particularly of the  $2l4l'$

configurations, and for some of the levels their results are the same (i.e. non degenerate) – see for example: the  $2s4f^3F_{2,3,4}^o$  levels. Also included in the table, for comparison purpose, are energies obtained from the *Flexible Atomic Code* (FAC) code of Gu (2008). These results listed under FAC1 include the same CI (configuration interaction) as in GRASP.

The inclusion of the Breit and QED effects (GRASP2) does not significantly alter the energies obtained with their exclusion (GRASP1), as both sets of results agree within 0.01 Ryd, and their orderings are also the same. Similarly, there is no discrepancy in the ordering of levels between GRASP and NIST, and the energy differences for common levels are generally within 0.01 Ryd. However, particularly for two levels, namely  $2p3s^1P_1^o$  and  $2p3d^1F_3^o$ , the NIST energies are higher by up to 0.06 Ryd. For some of the levels, including  $2p3s^1P_1^o$ , the NIST energies are not highly accurate as they have placed a question mark on these.

Our FAC1 energies show the same ordering as those of GRASP and NIST, and agree with our GRASP2 calculations within 0.05 Ryd. The inclusion of the  $2l5l'$  configurations, labelled FAC2 calculations in Table 1, makes no appreciable difference. Small discrepancies in the GRASP and FAC energies, also noted for several other ions, are primarily due to the different ways that the calculations of central potential for radial orbitals and recoupling schemes of angular parts have been performed – see the detailed discussion in the FAC manual (<http://sprg.ssl.berkeley.edu/~mfgu/fac/>). However, for the levels in common our GRASP2 energies are slightly closer to those of NIST than those from FAC. Therefore, based on the comparisons shown, our GRASP2 energy levels listed in Table 1 are assessed to be accurate to better than 0.3%.

## 3 RADIATIVE RATES

Since the A- values of Zhang & Sampson (1992) are limited to E1 transitions among the lowest 10 levels of Al X, we here provide a complete set of data for all transitions among the 98 levels. Furthermore, A- values are calculated for four types of transitions, namely electric dipole (E1), electric quadrupole (E2), magnetic dipole (M1), and magnetic quadrupole (M2). Generally, E1 transitions are dominant, but occasionally other types of transitions are also prominent and are therefore required for a complete plasma model. The absorption oscillator strength ( $f_{ij}$ ) and radiative rate  $A_{ji}$  (in  $s^{-1}$ ) for all types of transition  $i \rightarrow j$  are related by the following expression (Garstang 1968):

$$f_{ij} = \frac{mc}{8\pi^2 e^2} \lambda_{ji}^2 \frac{\omega_j}{\omega_i} A_{ji} = 1.49 \times 10^{-16} \lambda_{ji}^2 (\omega_j/\omega_i) A_{ji} \quad (1)$$

where  $m$  and  $e$  are the electron mass and charge, respectively,  $c$  the velocity of light,  $\lambda_{ji}$  the transition energy/wavelength in  $\text{\AA}$ , and  $\omega_i$  and  $\omega_j$  the statistical weights of the lower ( $i$ ) and upper ( $j$ ) levels, respectively. However, the relationships between oscillator strength  $f_{ij}$  (dimensionless) and the line strength  $S$  (in atomic unit, 1 a.u. =  $6.460 \times 10^{-36} \text{ cm}^2 \text{ esu}^2$ ) with the A- values are different for different types of transitions – see Eqs. (2–5) of Aggarwal & Keenan (2012c).

In Table 2 we list transition energies/wavelengths ( $\lambda$ , in  $\text{\AA}$ ), radiative rates ( $A_{ji}$ , in  $s^{-1}$ ), oscillator strengths ( $f_{ij}$ ,

dimensionless), and line strengths (S, in a.u.) for all 1468 electric dipole (E1) transitions among the 98 levels of Al X. For conciseness, results are only listed in the length form, which are considered to be more accurate. However, below we discuss the velocity/length form ratio, as this provides some assessment of the accuracy of the results. Also note that the *indices* used to represent the lower and upper levels of a transition are defined in Table 1. There are 1754 electric quadrupole (E2), 1424 magnetic dipole (M1), and 1792 magnetic quadrupole (M2) transitions among the same 98 levels. However, for these only the A-values are listed in Table 2, and the corresponding results for f-values can be easily obtained through Eq. (1).

As noted in section 1, f-values for Al X are available in the literature (Zhang & Sampson 1992) for only a limited number of transitions. Therefore, as with energy levels we have also performed a calculation with the FAC code of Gu (2008). Our calculated f-values from both GRASP and FAC, as well as their ratio, are listed in Table 3 for some representative transitions among the lowest 20 levels of Al X. For these transitions the agreement between the two sets of f-values is better than 20%, particularly for the strong ones with  $f \geq 0.01$ . However, there are 4 exceptions, namely 21–71 ( $2p3s\ ^3P_0^o - 2p4p\ ^3P_1$ ), 31–85 ( $2p3p\ ^3P_1 - 2p4d\ ^3P_2^o$ ), 46–76 ( $2p3d\ ^1P_1^o - 2p4p\ ^1D_2$ ), and 46–82 ( $2p3d\ ^1P_1^o - 2p4f\ ^3F_2$ ), for which the discrepancies are larger, but still less than 50%. These discrepancies are partly due to the corresponding differences in the energy levels of the two calculations.

A general criterion to assess the accuracy of f- or A-values is to compare the ratio of their length and velocity forms. This should ideally be close to unity but often is not, because the two formulations are not exactly the same. Therefore, we also include in Table 3 the ratio of the velocity and length forms. For a majority (89%) of the strong E1 transitions ( $f \geq 0.01$ ) the ratio is within 20% of unity, but discrepancies for some are higher, although mostly within a factor of two. However, for a few ( $\sim 8\%$ ) weak(er) transitions ( $f \leq 10^{-3}$ ) the two forms of the f-value differ by up to several orders of magnitude – see for example: 34–37, 56–58, 67–75, and 71–73. For all of these transitions,  $\Delta E_{ij}$  is very low and a small variation in this has a large effect on the f-value. A few other transitions with significant  $\Delta E_{ij}$  for which the two forms disagree by over 20% are: 3–12 ( $f \sim 10^{-6}$ ), 6–15 ( $f \sim 10^{-3}$ ), and 10–15 ( $f \sim 10^{-5}$ ), as shown in Table 3. Finally, as noted for the energy levels in section 2, inclusion of additional CI with the  $n = 5$  configurations does not make any appreciable effect on the f- or A-values. To be specific, discrepancies in A-values for all strong E1 transitions are less than  $\sim 20\%$  with those listed in Tables 2 and 3. Therefore, based on this and other comparisons already discussed, we are confident that for almost all strong E1 transitions listed in Table 2, our f-values (and other related parameters) are accurate to better than 20%. However, for the weaker E1 and other types of transitions (i.e. E2, M1 and M2) the accuracy may be comparatively lower. Finally, we note that these conclusions are similar to those arrived earlier for transitions of another Be-like ion, i.e. Ti XIX (Aggarwal & Keenan 2012c).

#### 4 LIFETIMES

The lifetime  $\tau$  for a level  $j$  is defined as follows (Woodgate 1970):

$$\tau_j = \frac{1}{\sum_i A_{ji}}. \quad (2)$$

Since this is a measurable quantity, it facilitates an assessment of the accuracy of the A-values. Therefore, in Table 1 we have also listed our calculated lifetimes. Generally, A-values for E1 transitions dominate, but for higher accuracy we have also included the contributions from E2, M1 and M2. Their inclusion is particularly useful for those levels which do not connect via E1 transitions. Träbert & Heckmann (1980) have measured the lifetime of the  $2s2p\ ^1P_1^o$  level to be  $175 \pm 15$  ps, which compares very well with our result of 160 ps and the 173 ps theoretical value of Andersson et al. (2009). They have also measured lifetimes corresponding to the  $2s2p\ ^1P_1^o - 2p^2\ ^1D_2$  (5–9) and  $2s2p\ ^1P_1^o - 2p^2\ ^1S_0$  (5–10) transitions to be  $1080 \pm 80$  and  $112 \pm 12$  ps, respectively, which compare favourably with our results of 1072 and 105 ps, respectively.

#### 5 COLLISION STRENGTHS

The collision strength for electron impact excitation ( $\Omega$ ) is related to the better-known parameter collision cross section ( $\sigma_{ij}$ ,  $\pi a_0^2$ ) by the following equation (Burgess & Tully 1992):

$$\Omega_{ij}(E) = k_i^2 \omega_i \sigma_{ij}(E) \quad (3)$$

where  $k_i^2$  is the incident energy of the electron and  $\omega_i$  is the statistical weight of the initial state. Since  $\Omega$  is a symmetric and dimensionless quantity, results for it are preferred over those of  $\sigma_{ij}$ .

As in our earlier work, such as on Ti XIX (Aggarwal & Keenan 2012c), for calculating  $\Omega$  we have adopted the *Dirac Atomic R-matrix Code* (DARC) of P. H. Norrington and I. P. Grant, available at the website <http://web.am.qub.ac.uk/DARC/>. This code includes the relativistic effects, which are very important for high Z ions, but are equally significant for taking into account degeneracy among the fine-structure levels of a state of an ion with lower Z, such as Al X. The DARC code is based on the *jj* coupling scheme and uses the Dirac-Coulomb Hamiltonian in an *R*-matrix approach. The *R*-matrix radius adopted for Al X is 6.4 au, and 55 continuum orbitals have been included for each channel angular momentum in the expansion of the wavefunction. This large expansion is computationally more demanding but allows us to compute  $\Omega$  up to an energy of 380 Ryd,  $\sim 355$  Ryd above the highest threshold considered in this work. Furthermore, this large energy range is sufficient to calculate values of effective collision strength  $\Upsilon$  (see section 6) up to  $T_e = 1.8 \times 10^7$  K, more than an order of magnitude higher than the temperature of maximum abundance in ionisation equilibrium for Al X, i.e.  $1.3 \times 10^6$  K (Bryans, Landi & Savin 2009). The maximum number of channels for a partial wave is 428 and the corresponding size of the Hamiltonian matrix is 23,579. To achieve convergence of  $\Omega$  for a majority of transitions and at all energies, we have included all partial waves with angular momentum  $J \leq 40.5$ . Additionally, to account for higher

neglected partial waves, we have included a top-up, based on the Coulomb-Bethe (Burgess & Sheorey 1974) and geometric series approximations for allowed and forbidden transitions, respectively. These contributions enhance the accuracy of our calculated values of  $\Omega$ s, particularly at the higher end of the energy range.

In Table 4 we list our values of  $\Omega$  for resonance transitions of Al X at energies *above* thresholds. The indices used to represent the levels of a transition have already been defined in Table 1. Unfortunately, no similar data are available for comparison purposes as already noted in section 1. One way to assess the accuracy of these results is to compare with the similar calculations from FAC, as undertaken in our work on Ti XIX (Aggarwal & Keenan 2012c). However, such a comparison is not very useful, particularly for the forbidden transitions, because often there are anomalies in the FAC calculations, as shown in Fig. 6 of Aggarwal & Keenan (2012a,b). Nevertheless, our listed results for  $\Omega$  should be helpful for future comparisons.

## 6 EFFECTIVE COLLISION STRENGTHS

As well as energy levels and radiative rates, excitation and de-excitation rates are required for plasma modelling, which are determined from the collision strengths ( $\Omega$ ). However,  $\Omega$  does not vary smoothly with increasing energy, particularly at energies in between the thresholds. The threshold energy region is generally dominated by numerous closed-channel (Feshbach) resonances, especially for (semi) forbidden transitions. Therefore, values of  $\Omega$  should be calculated in a fine energy mesh to accurately account for their contribution. Additionally, in many plasmas electrons have a wide distribution of velocities, and therefore it is more appropriate to average values of  $\Omega$  over a suitable distribution. For astrophysical applications the most appropriate and commonly used distribution is *Maxwellian*, although any other distribution may also be applied if suitable for a particular plasma. Such an averaged value, known as *effective* collision strength ( $\Upsilon$ ) (Burgess & Tully 1992) is:

$$\Upsilon(T_e) = \int_0^\infty \Omega(E) \exp(-E_j/kT_e) d(E_j/kT_e), \quad (4)$$

where  $k$  is Boltzmann constant,  $T_e$  electron temperature in K, and  $E_j$  the electron energy with respect to the final (excited) state. Once the value of  $\Upsilon$  is known the corresponding results for the excitation  $q(i,j)$  and de-excitation  $q(j,i)$  rates can be easily obtained from the following equations:

$$q(i,j) = \frac{8.63 \times 10^{-6}}{\omega_i T_e^{1/2}} \Upsilon \exp(-E_{ij}/kT_e) \quad \text{cm}^3 \text{s}^{-1} \quad (5)$$

and

$$q(j,i) = \frac{8.63 \times 10^{-6}}{\omega_j T_e^{1/2}} \Upsilon \quad \text{cm}^3 \text{s}^{-1}, \quad (6)$$

where  $\omega_i$  and  $\omega_j$  are the statistical weights of the initial ( $i$ ) and final ( $j$ ) states, respectively, and  $E_{ij}$  is the transition energy. The contribution of resonances often enhances the values of  $\Upsilon$  over those of the background collision strengths ( $\Omega_B$ ), particularly for the (semi) forbidden transitions. This enhancement can be dominant (by up to an order of magnitude or even more), but depends on the type of a transi-

tion as well as the temperature. Generally, the enhancement in  $\Upsilon$  is greater at lower temperatures. Similarly, values of  $\Omega$  should be calculated over a wide energy range (above thresholds) to obtain convergence of the integral in Eq. (4), as demonstrated in Fig. 7 of Aggarwal & Keenan (2008). If calculations of  $\Omega$  are performed only for a limited range of energy, it is still necessary to include the contribution of  $\Omega$  at high energies. For this the high energy limits recommended by Burgess & Tully (1992) for a range of transitions may be adopted. However, in our work there is no such need because calculations for  $\Omega$  have already been performed up to sufficiently high energies, as clarified in section 5.

To delineate resonances, we have performed our calculations of  $\Omega$  at over  $\sim 13,000$  energies in the thresholds region. Close to thresholds ( $\sim 0.1$  Ryd above a threshold) the energy mesh is 0.001 Ryd, and away from thresholds is 0.002 Ryd. This fine resolution accounts for the majority of resonances, and their density and importance can be appreciated from transitions of Ti XIX shown in Figs. 7–12 of Aggarwal & Keenan (2012c). For transitions of Al X we observe similar dense resonances, as shown in Figs. 1 and 2 for two important lines, namely  $2s^2 \ ^1S_0 - 2s2p \ ^3P_1^o$  (1–3) and  $2s2p \ ^3P_1^o - 2p^2 \ ^1D_2$  (3–9). Both of these are allowed transitions in  $jj$  coupling and yet resonances are not only dense but also highly significant in magnitude. Furthermore, resonances are spread over a range of 20 Ryd (equivalently over  $3 \times 10^6$  K), and hence make an appreciable contribution to  $\Upsilon$  over the entire range of temperatures of interest for transitions of Al X.

Our calculated values of  $\Upsilon$  are listed in Table 5 over a wide temperature range up to  $10^{7.2}$  K, suitable for applications to a wide range of laboratory and astrophysical plasmas. Corresponding data at any desired temperature can either be easily interpolated, because  $\Upsilon$  is a slowly varying function of  $T_e$ , or may be requested from the first author. As noted in section 1, Keenan et al. (1986) have reported values of  $\Upsilon$  for transitions among the lowest 10 levels of Al X. In Table 6 we compare results for  $\Upsilon$  at three temperatures of  $10^{5.9}$ ,  $10^{6.1}$  and  $10^{6.3}$  K, which are most relevant for Al X (Bryans et al. 2009). The interpolated values of  $\Upsilon$  listed by Keenan et al. are based on the  $R$ -matrix calculations for C III, O V, Ne VII and Si XI, which were performed in  $LS$  coupling. Since their work is not based on direct calculations for Al X, differences with their results are not unexpected. For transitions which are allowed in  $LS$  coupling, such as 1–5 and 5–9/10, there is no discrepancy between our results and those of Keenan et al. This is because such allowed transitions do not normally have a significant contribution from resonances. However, there are differences between the two sets of  $\Upsilon$  of up a factor of two for several (but not all) transitions which are allowed in  $LS$  coupling but not in  $jj$ , such as 2/3/4–6/7/8, i.e.  $2s2p \ ^3P_{0,1,2}^o - 2p^2 \ ^3P_{0,1,2}$ . For other transitions (particularly forbidden) the  $\Upsilon$  values of Keenan et al. are *underestimated* by up to a factor of 4.

## 7 CONCLUSIONS

Energies and lifetimes for the lowest 98 levels of Al X belonging to the  $n \leq 4$  configurations have been reported, for which the GRASP code has been adopted. Also listed are results for radiative rates for four types of transitions (E1, E2,

M1 and M2). Based on a variety of comparisons with available measurements, as well as with analogous calculations with the FAC code, our results for radiative rates, oscillator strengths and line strengths are judged to be accurate to better than 20% for a majority of strong transitions. Similarly, energy levels are assessed to be accurate to  $\sim 0.3\%$ . Measurements of lifetimes are available for only three levels for which there are no discrepancies with theory.

Results have also been reported for collision strengths over a wide range of energy, but only for resonance transitions. However, corresponding results for effective collision strengths are listed for *all* transitions among the 98 levels of Al X and over a wide range of temperature, suitable for applications in a variety of plasmas. For calculations of  $\Upsilon$ , resonances in the thresholds energy region for many transitions are noted to be as dominant as for Ti XIX (Aggarwal & Keenan 2012c). Their inclusion in the determination of  $\Upsilon$  has significantly enhanced the results. Since no prior calculations with comparable accuracy and complexity are available, it is not straightforward to assess the uncertainty of our values of  $\Upsilon$ . However, comparisons between our results and those interpolated by Keenan et al. (1986) have been made for transitions among the lowest 10 levels, and the latter are found to be underestimated by up to a factor of four for several transitions, mostly forbidden.

Since a large range of partial waves has been considered to achieve convergence of  $\Omega$  at all energies and contribution of higher neglected partial waves has been included, our results for  $\Omega$  should be accurate to better than 20%. This assessment of accuracy is mainly based on comparisons of similar data for Be-like ion of Ti. Similarly, to calculate values of  $\Upsilon$  up to  $T_e = 10^{7.2}$  K, we have included a wide energy range for  $\Omega$  and have also resolved resonances in a fine energy mesh to account for their contribution. Hence, we see no apparent limitations in our data. Moreover, as for Ti XIX (Aggarwal & Keenan 2012c), we estimate the accuracy of our results for  $\Upsilon$  to be better than 20% for most transitions. However, there is scope for improvement, especially for transitions involving levels of the  $n = 4$  configurations. This can perhaps be achieved by the inclusion of levels of the  $n = 5$  configurations in the collisional calculations. At present we believe the reported results for radiative and excitation rates for transitions in Al X are the most exhaustive and accurate available to date. The complete set of atomic data should be highly useful for modelling astrophysical and fusion plasmas.

## ACKNOWLEDGMENTS

KMA is thankful to AWE Aldermaston for financial support.

## REFERENCES

- Aggarwal K. M., Keenan F. P., 2004, Phys. Scr., 69, 176  
 Aggarwal K. M., Keenan F. P., 2008, Eur. Phys. J., D 46, 205  
 Aggarwal K. M., Keenan F. P., 2012a, Phys. Scr., 85, 025305  
 Aggarwal K. M., Keenan F. P., 2012b, Phys. Scr., 85, 025306

- Aggarwal K. M., Keenan F. P., 2012c, Phys. Scr., 86, 055301  
 Aggarwal K. M., Keenan F. P., 2013, Phys. Scr., 87, 055302  
 Aggarwal K. M., Keenan F. P., Lawson K. D., 2008, At. Data Nucl. Data Tables, 94, 323  
 Aggarwal K. M., Keenan F. P., Lawson K. D., 2010, At. Data Nucl. Data Tables, 96, 123  
 Aggarwal K. M., Tayal V., Gupta G. P., Keenan F. P., 2007, At. Data Nucl. Data Tables, 93, 615  
 Andersson M., Zou Y., Hutton R., Brage T., 2009, Phys. Rev. A 79, 032501  
 Bar-Shalom A., Klapisch M. Oreg, J., 2001, J. Quant. Spect. Rad. Trans., 71, 169  
 Bryans P., Landi E., Savin D. W., 2009, ApJ, 691, 1540  
 Burgess A., Sheorey V. B., 1974, J. Phys., B7, 2403  
 Burgess A., Tully J. A., 1992, A&A, 254, 436  
 Garstang R. H., 1968, J. Phys., B1, 847  
 Grant I. P., McKenzie B. J., Norrington P. H., Mayers D. F., Pyper N. C., 1980, Comput. Phys. Commun., 21, 207  
 Gu M. F., 2008, Can. J. Phys., 86, 675  
 Gu M. F., Beiersdorfer P., Lepson J. K., 2011, ApJ, 732, 91  
 Keenan F. P., Berrington K. A., Burke P. G., Dufton P. L., Kingston A. E., 1986, Phys. Scr., 34, 216  
 Landi E., Doron R., Feldman U., Doscheck G. A., 2001, ApJ, 556, 912  
 Martin W. C., Zalubas R., 1979, J. Phys. Chem. Ref. Data, 8, 817  
 Träbert E., Heckmann P. H., 1980, Phys. Scr., 22, 489  
 Wilhelm K. et al., 1995, Sol. Phys., 162, 189  
 Woodgate G. K., 1970 *Elementary Atomic Structure*, New York: McGraw-Hill  
 Zhang H., Sampson D. H., 1992, At. Data Nucl. Data Tables, 52, 143

**Table 1.** Energy levels (in Ryd) of Al X and their lifetimes.

Index	Configuration	Level	NIST	GRASP1	GRASP2	FAC1	FAC2	$\tau$ (s)
1	2s <sup>2</sup>	<sup>1</sup> S <sub>0</sub>	0.00000	0.00000	0.00000	0.00000	0.00000	.....
2	2s2p	<sup>3</sup> P <sub>0</sub> <sup>o</sup>	1.41381	1.41694	1.41897	1.42722	1.42661	.....
3	2s2p	<sup>3</sup> P <sub>1</sub> <sup>o</sup>	1.42885	1.43399	1.43387	1.44188	1.44128	5.963-06
4	2s2p	<sup>3</sup> P <sub>2</sub> <sup>o</sup>	1.46194	1.46944	1.46662	1.47416	1.47357	1.246-00
5	2s2p	<sup>1</sup> P <sub>1</sub> <sup>o</sup>	2.73827	2.81662	2.81633	2.81532	2.81053	1.600-10
6	2p <sup>2</sup>	<sup>3</sup> P <sub>0</sub>	3.68675	3.71751	3.71907	3.73711	3.73633	2.154-10
7	2p <sup>2</sup>	<sup>3</sup> P <sub>1</sub>	3.70446	3.73616	3.73652	3.75430	3.75353	2.129-10
8	2p <sup>2</sup>	<sup>3</sup> P <sub>2</sub>	3.73337	3.76904	3.76518	3.78247	3.78171	2.096-10
9	2p <sup>2</sup>	<sup>1</sup> D <sub>2</sub>	4.09826	4.17709	4.17504	4.19138	4.18716	1.050-09
10	2p <sup>2</sup>	<sup>1</sup> S <sub>0</sub>	5.04644	5.17695	5.17938	5.18781	5.18508	1.052-10
11	2s3s	<sup>3</sup> S <sub>1</sub>	16.9109	16.90263	16.89542	16.89461	16.89432	5.201-12
12	2s3s	<sup>1</sup> S <sub>0</sub>	17.1721	17.16367	17.15693	17.17011	17.16978	1.435-11
13	2s3p	<sup>1</sup> P <sub>1</sub> <sup>o</sup>	17.5314	17.53546	17.52796	17.53879	17.53775	2.139-12
14	2s3p	<sup>3</sup> P <sub>0</sub> <sup>o</sup>		17.55638	17.55008	17.56230	17.56240	4.322-10
15	2s3p	<sup>3</sup> P <sub>1</sub> <sup>o</sup>		17.56265	17.55555	17.56749	17.56755	4.143-11
16	2s3p	<sup>3</sup> P <sub>2</sub> <sup>o</sup>		17.57084	17.56323	17.57501	17.57512	4.037-10
17	2s3d	<sup>3</sup> D <sub>1</sub>	17.9142	17.91422	17.90599	17.92123	17.91911	1.076-12
18	2s3d	<sup>3</sup> D <sub>2</sub>	17.9162	17.91616	17.90756	17.92272	17.92059	1.079-12
19	2s3d	<sup>3</sup> D <sub>3</sub>	17.9182	17.91907	17.91022	17.92529	17.92316	1.084-12
20	2s3d	<sup>1</sup> D <sub>2</sub>	18.1555	18.18722	18.17882	18.19304	18.18938	1.608-12
21	2p3s	<sup>3</sup> P <sub>0</sub> <sup>o</sup>		18.69695	18.69110	18.71734	18.71745	6.603-12
22	2p3s	<sup>3</sup> P <sub>1</sub> <sup>o</sup>		18.71325	18.70615	18.73218	18.73226	6.538-12
23	2p3s	<sup>3</sup> P <sub>2</sub> <sup>o</sup>	18.7460	18.75178	18.74171	18.76709	18.76720	6.422-12
24	2p3s	<sup>1</sup> P <sub>1</sub> <sup>o</sup>	19.0625	19.01237	19.00401	19.03602	19.03186	5.332-12
25	2p3p	<sup>1</sup> P <sub>1</sub>	19.0894	19.09350	19.08552	19.11202	19.11216	3.777-12
26	2p3p	<sup>3</sup> D <sub>1</sub>	19.1578	19.16750	19.16008	19.18591	19.18569	7.090-12
27	2p3p	<sup>3</sup> D <sub>2</sub>	19.1721	19.18332	19.17515	19.20029	19.20005	7.590-12
28	2p3p	<sup>3</sup> D <sub>3</sub>	19.0240	19.21937	19.20844	19.23319	19.23295	7.516-12
29	2p3p	<sup>3</sup> S <sub>1</sub>	19.3160	19.33016	19.32141	19.34755	19.34700	4.454-12
30	2p3p	<sup>3</sup> P <sub>0</sub>		19.39104	19.38473	19.43306	19.43188	4.346-12
31	2p3p	<sup>3</sup> P <sub>1</sub>	19.3980	19.40812	19.40025	19.44680	19.44568	4.348-12
32	2p3p	<sup>3</sup> P <sub>2</sub>	19.4137	19.42677	19.41709	19.46398	19.46286	4.347-12
33	2p3d	<sup>3</sup> F <sub>2</sub> <sup>o</sup>		19.47683	19.46968	19.50477	19.50257	1.062-11
34	2p3d	<sup>3</sup> F <sub>3</sub> <sup>o</sup>		19.50513	19.49594	19.53497	19.53229	1.144-10
35	2p3d	<sup>1</sup> D <sub>2</sub> <sup>o</sup>	19.5155	19.52021	19.50998	19.54890	19.54802	3.121-12
36	2p3d	<sup>3</sup> F <sub>4</sub> <sup>o</sup>		19.53388	19.52225	19.55770	19.55499	2.471-09
37	2p3p	<sup>1</sup> D <sub>2</sub>	19.5778	19.61598	19.60698	19.66078	19.65660	2.935-12
38	2p3d	<sup>3</sup> D <sub>1</sub> <sup>o</sup>	19.6893	19.69761	19.68861	19.72802	19.72823	8.663-13
39	2p3d	<sup>3</sup> D <sub>2</sub> <sup>o</sup>	19.7012	19.70542	19.69591	19.73859	19.73878	8.831-13
40	2p3d	<sup>3</sup> D <sub>3</sub> <sup>o</sup>	19.7138	19.72105	19.70995	19.75056	19.75077	8.622-13
41	2p3d	<sup>3</sup> P <sub>2</sub> <sup>o</sup>	19.7762	19.79012	19.77978	19.81691	19.81661	1.553-12
42	2p3d	<sup>3</sup> P <sub>1</sub> <sup>o</sup>	19.7898	19.80156	19.79099	19.82829	19.82796	1.579-12
43	2p3d	<sup>3</sup> P <sub>0</sub> <sup>o</sup>		19.80750	19.79743	19.83558	19.83523	1.606-12
44	2p3p	<sup>1</sup> S <sub>0</sub>		19.94986	19.94280	20.00059	19.98775	5.527-12
45	2p3d	<sup>1</sup> F <sub>3</sub> <sup>o</sup>	19.9828	20.03858	20.02755	20.06982	20.06305	7.032-13
46	2p3d	<sup>1</sup> P <sub>1</sub> <sup>o</sup>		20.08601	20.07597	20.11448	20.11208	1.174-12
47	2s4s	<sup>3</sup> S <sub>1</sub>		22.54933	22.54097	22.54646	22.54537	1.037-11
48	2s4s	<sup>1</sup> S <sub>0</sub>		22.65071	22.64271	22.65172	22.64843	1.106-11

**Table 1.** Energy levels (in Ryd) of Al X and their lifetimes.

Index	Configuration	Level	NIST	GRASP1	GRASP2	FAC1	FAC2	$\tau$ (s)
49	2s4p	$^3P_0^o$		22.79976	22.79178	22.80264	22.80264	3.219-11
50	2s4p	$^3P_1^o$		22.80151	22.79331	22.80412	22.80410	3.045-11
51	2s4p	$^3P_2^o$		22.80575	22.79723	22.80786	22.80787	3.258-11
52	2s4p	$^1P_1^o$		22.83208	22.82350	22.83676	22.83426	3.598-12
53	2s4d	$^3D_1$		22.94439	22.93591	22.94425	22.94326	2.738-12
54	2s4d	$^3D_2$		22.94507	22.93645	22.94479	22.94380	2.743-12
55	2s4d	$^3D_3$		22.94610	22.93741	22.94574	22.94474	2.750-12
56	2s4d	$^1D_2$	23.0328	23.03637	23.02777	23.03406	23.03223	3.107-12
57	2s4f	$^3F_2^o$	23.0420	23.03790	23.02937	23.03614	23.03421	6.766-12
58	2s4f	$^3F_3^o$	23.0420	23.03825	23.02961	23.03639	23.03446	6.766-12
59	2s4f	$^3F_4^o$	23.0420	23.03872	23.03003	23.03679	23.03485	6.767-12
60	2s4f	$^1F_3^o$		23.06257	23.05392	23.06192	23.05970	6.749-12
61	2p4s	$^3P_0^o$		24.21374	24.20663	24.23547	24.23546	1.115-11
62	2p4s	$^3P_1^o$		24.22541	24.21768	24.24657	24.24586	1.071-11
63	2p4s	$^3P_2^o$		24.26942	24.25816	24.28604	24.28604	1.066-11
64	2p4s	$^1P_1^o$		24.33218	24.32131	24.35227	24.34046	7.459-12
65	2p4p	$^1P_1$		24.39368	24.38599	24.41716	24.41709	5.881-12
66	2p4p	$^3D_1$		24.42626	24.41706	24.44825	24.44790	6.445-12
67	2p4p	$^3D_2$		24.42918	24.42038	24.45195	24.45182	7.901-12
68	2p4p	$^3D_3$		24.46580	24.45399	24.48457	24.48453	7.977-12
69	2p4p	$^3S_1$		24.48873	24.47906	24.51326	24.50573	6.182-12
70	2p4p	$^3P_0$		24.49044	24.48248	24.52186	24.52000	7.285-12
71	2p4p	$^3P_1$		24.52093	24.50993	24.54626	24.54261	6.635-12
72	2p4p	$^3P_2$		24.52528	24.51423	24.55234	24.55105	7.233-12
73	2p4d	$^3F_2^o$		24.53974	24.53225	24.56341	24.56166	9.250-12
74	2p4d	$^3F_3^o$		24.56480	24.55592	24.58731	24.58512	1.027-11
75	2p4d	$^1D_2^o$		24.57451	24.56504	24.59586	24.59471	5.064-12
76	2p4d	$^1D_2$	24.5755	24.59319	24.58233	24.62476	24.61978	5.473-12
77	2p4d	$^3F_4^o$		24.59736	24.58565	24.61617	24.61389	1.423-11
78	2p4d	$^3D_1^o$		24.61927	24.61082	24.64026	24.63980	2.096-12
79	2p4d	$^3D_2^o$		24.63018	24.62033	24.65013	24.64908	2.414-12
80	2p4f	$^1F_3$		24.63738	24.62916	24.65589	24.65263	6.803-12
81	2p4f	$^3F_3$		24.64055	24.63240	24.65934	24.65823	6.938-12
82	2p4f	$^3F_2$		24.64195	24.63346	24.66072	24.66063	6.880-12
83	2p4f	$^3F_4$		24.64430	24.63607	24.66310	24.65907	7.045-12
84	2p4d	$^3D_3^o$		24.64876	24.63750	24.66663	24.66666	2.100-12
85	2p4d	$^3P_2^o$		24.67077	24.65945	24.68876	24.68505	2.914-12
86	2p4d	$^3P_1^o$		24.67783	24.66650	24.69593	24.69122	3.141-12
87	2p4d	$^3P_0^o$		24.68175	24.67065	24.70015	24.69477	3.344-12
88	2p4f	$^3G_3$		24.68824	24.67701	24.70310	24.69764	6.913-12
89	2p4f	$^3G_4$		24.69295	24.68171	24.70791	24.70163	7.024-12
90	2p4f	$^3G_5$		24.70949	24.69767	24.72356	24.71287	6.980-12
91	2p4f	$^3D_3$		24.71783	24.70694	24.73342	24.75159	6.831-12
92	2p4f	$^3D_2$		24.72363	24.71272	24.73956	24.73334	6.818-12
93	2p4f	$^1G_4$		24.72378	24.71209	24.73907	24.72144	7.701-12
94	2p4f	$^3D_1$		24.73681	24.72532	24.75171	24.72754	6.820-12
95	2p4p	$^1S_0$		24.74104	24.73058	24.78352	24.73931	1.064-11
96	2p4f	$^1D_2$		24.74808	24.73671	24.76430	24.76358	6.805-12
97	2p4d	$^1F_3^o$		24.77573	24.76474	24.79181	24.77893	1.472-12
98	2p4d	$^1P_1^o$		24.78736	24.77677	24.80363	24.79443	2.300-12

NIST: <http://www.nist.gov/pml/data/asd.cfm>

GRASP1: Coulomb energies

GRASP2: QED corrected energies

FAC1: Energies from the FAC for 98 level calculations

FAC2: Energies from the FAC for 166 level calculations

**Table 3.** Comparison between GRASP and FAC f- values for some transitions of Al X. ( $a \pm b \equiv a \times 10^{\pm b}$ ).

$i$	$j$	f (GRASP)	f (FAC)	Vel./Len.	f(GRASP)/f(FAC)
1	3	3.046-5	3.039-5	0.70	1.00
1	5	2.942-1	2.942-1	0.97	1.00
1	13	5.324-1	5.445-1	0.97	0.98
1	15	2.478-2	2.183-2	0.97	1.14
2	7	1.124-1	1.127-1	0.90	1.00
2	11	3.321-2	3.394-2	0.94	0.98
2	17	7.100-1	7.095-1	0.98	1.00
3	6	3.688-2	3.698-2	0.90	1.00
3	7	2.790-2	2.797-2	0.90	1.00
3	8	4.719-2	4.731-2	0.91	1.00
3	9	2.755-5	2.640-5	0.61	1.04
3	10	4.082-6	4.097-6	1.70	1.00
3	11	3.334-2	3.404-2	0.94	0.98
3	12	1.076-6	1.377-6	0.46	0.78
3	17	1.775-1	1.773-1	0.98	1.00
3	18	5.318-1	5.315-1	0.98	1.00
4	7	2.743-2	2.751-2	0.90	1.00
4	8	8.326-2	8.348-2	0.90	1.00
4	9	3.187-4	3.139-4	0.93	1.02
4	11	3.356-2	3.423-2	0.94	0.98
4	17	7.105-3	7.107-3	0.98	1.00
4	18	1.064-1	1.063-1	0.98	1.00
4	19	5.947-1	5.945-1	0.98	1.00
5	8	1.638-4	1.632-4	1.50	1.00
5	9	1.048-1	1.061-1	1.30	0.99
5	10	7.063-2	7.054-2	0.58	1.00
5	12	1.406-2	1.456-2	0.79	0.97
5	20	5.462-1	5.424-1	1.00	1.01
6	15	1.296-3	1.365-3	1.70	0.95
7	14	4.245-4	4.460-4	1.70	0.95
7	15	2.922-4	3.098-4	1.70	0.94
7	16	6.034-4	6.250-4	1.60	0.97
8	13	1.141-4	1.106-4	0.96	1.03
8	15	2.565-4	2.766-4	1.80	0.93
8	16	1.004-3	1.048-3	1.70	0.96
9	13	1.181-2	1.201-2	0.62	0.98
9	15	6.397-4	5.647-4	0.66	1.13
9	16	1.847-6	2.138-6	1.90	0.86
10	13	2.320-3	1.955-3	0.26	1.19
10	15	8.195-5	5.692-5	0.15	1.44
11	14	3.051-2	3.080-2	1.10	0.99
11	15	8.808-2	8.943-2	1.10	0.98
11	16	1.560-1	1.573-1	1.10	0.99
13	20	1.154-1	1.155-1	0.79	1.00



**Table 4.** Collision strengths for resonance transitions in Al X. ( $a\pm b \equiv a \times 10^{\pm b}$ ).

Transition		Energy (Ryd)						
$i$	$j$	50	100	150	200	250	300	350
1	2	1.708-3	6.687-4	3.528-4	2.180-4	1.481-4	1.070-4	8.115-5
1	3	5.675-3	2.584-3	1.630-3	1.195-3	9.725-4	8.336-4	7.602-4
1	4	8.495-3	3.323-3	1.752-3	1.082-3	7.350-4	5.314-4	4.027-4
1	5	1.958+0	2.275+0	2.361+0	2.286+0	2.251+0	2.206+0	2.279+0
1	6	4.860-5	1.852-5	1.131-5	8.698-6	7.501-6	6.860-6	6.481-6
1	7	1.206-4	3.403-5	1.399-5	7.060-6	4.056-6	2.540-6	1.700-6
1	8	2.439-4	1.062-4	7.504-5	6.460-5	6.021-5	5.810-5	5.694-5
1	9	1.217-2	1.273-2	1.300-2	1.315-2	1.324-2	1.331-2	1.334-2
1	10	4.128-3	3.532-3	3.216-3	3.020-3	2.888-3	2.793-3	2.722-3
1	11	1.295-3	4.340-4	2.162-4	1.297-4	8.662-5	6.202-5	4.661-5
1	12	6.828-2	7.410-2	7.622-2	7.737-2	7.814-2	7.872-2	7.918-2
1	13	7.765-2	1.371-1	1.779-1	2.084-1	2.328-1	2.532-1	2.712-1
1	14	3.425-4	9.731-5	4.461-5	2.538-5	1.633-5	1.135-5	8.339-6
1	15	5.179-3	7.740-3	9.822-3	1.144-2	1.276-2	1.386-2	1.484-2
1	16	1.705-3	4.843-4	2.220-4	1.263-4	8.125-5	5.649-5	4.150-5
1	17	1.806-3	5.195-4	2.390-4	1.360-4	8.740-5	6.076-5	4.461-5
1	18	3.014-3	8.719-4	4.051-4	2.338-4	1.530-4	1.088-4	8.194-5
1	19	4.212-3	1.211-3	5.574-4	3.172-4	2.038-4	1.417-4	1.040-4
1	20	1.222-1	1.606-1	1.763-1	1.846-1	1.894-1	1.926-1	1.946-1
1	21	7.219-6	2.127-6	9.620-7	5.386-7	3.412-7	2.344-7	1.704-7
1	22	5.483-5	6.518-5	7.987-5	9.248-5	1.030-4	1.121-4	1.206-4
1	23	3.537-5	1.043-5	4.721-6	2.644-6	1.675-6	1.151-6	8.370-7
1	24	2.573-3	4.370-3	5.682-3	6.696-3	7.515-3	8.208-3	8.847-3
1	25	9.645-5	6.424-5	4.745-5	3.707-5	3.011-5	2.515-5	2.146-5
1	26	7.385-5	2.769-5	1.486-5	9.490-6	6.706-6	5.058-6	3.993-6
1	27	1.200-4	4.268-5	2.257-5	1.472-5	1.093-5	8.830-6	7.552-6
1	28	1.582-4	5.301-5	2.551-5	1.476-5	9.546-6	6.648-6	4.885-6
1	29	5.365-5	1.732-5	8.380-6	4.941-6	3.270-6	2.334-6	1.754-6
1	30	9.022-6	3.664-6	2.649-6	2.333-6	2.205-6	2.145-6	2.113-6
1	31	2.166-5	5.233-6	2.040-6	1.014-6	5.849-7	3.716-7	2.533-7
1	32	4.262-5	1.928-5	1.521-5	1.402-5	1.356-5	1.334-5	1.323-5
1	33	9.028-5	4.142-5	3.065-5	2.549-5	2.216-5	1.973-5	1.784-5
1	34	1.035-4	2.745-5	1.348-5	8.746-6	6.617-6	5.488-6	4.823-6
1	35	1.284-4	9.889-5	8.740-5	7.823-5	7.063-5	6.430-5	5.898-5
1	36	1.281-4	3.151-5	1.366-5	7.577-6	4.813-6	3.330-6	2.443-6
1	37	1.036-3	1.273-3	1.348-3	1.377-3	1.389-3	1.394-3	1.396-3
1	38	5.883-5	6.940-5	8.107-5	9.052-5	9.820-5	1.047-4	1.108-4
1	39	2.497-5	5.629-6	2.388-6	1.365-6	9.207-7	6.864-7	5.460-7
1	40	2.571-5	6.975-6	4.314-6	3.632-6	3.403-6	3.318-6	3.288-6
1	41	1.322-4	3.616-5	1.639-5	9.316-6	6.021-6	4.225-6	3.142-6
1	42	9.320-5	3.969-5	3.102-5	2.927-5	2.931-5	2.995-5	3.090-5
1	43	2.743-5	7.464-6	3.351-6	1.881-6	1.199-6	8.287-7	6.066-7
1	44	5.905-4	5.783-4	5.762-4	5.761-4	5.766-4	5.774-4	5.783-4
1	45	1.108-3	1.209-3	1.252-3	1.280-3	1.300-3	1.316-3	1.330-3
1	46	6.973-3	1.000-2	1.198-2	1.347-2	1.466-2	1.566-2	1.658-2
1	47	4.959-4	1.521-4	7.309-5	4.301-5	2.842-5	2.010-5	1.508-5
1	48	1.337-2	1.490-2	1.547-2	1.578-2	1.598-2	1.613-2	1.625-2
1	49	1.600-4	4.049-5	1.768-5	9.791-6	6.201-6	4.252-6	3.104-6
1	50	6.261-4	3.797-4	3.866-4	4.202-4	4.553-4	4.886-4	5.208-4

**Table 4.** Collision strengths for resonance transitions in Al X. ( $a \pm b \equiv a \times 10^{\pm b}$ ).

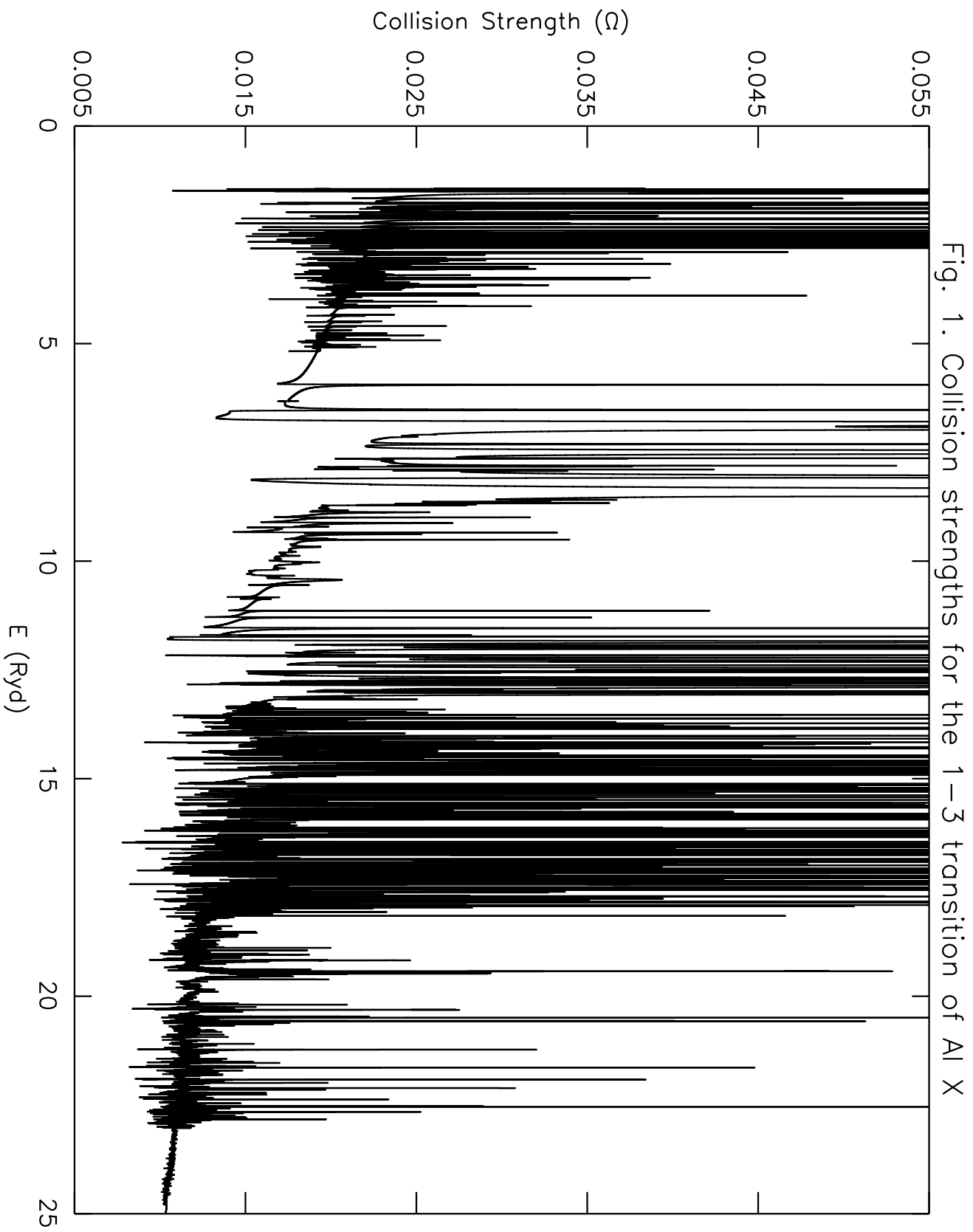
Transition		Energy (Ryd)						
<i>i</i>	<i>j</i>	50	100	150	200	250	300	350
1	51	7.968-4	2.016-4	8.798-5	4.874-5	3.086-5	2.116-5	1.545-5
1	52	1.720-2	2.989-2	3.864-2	4.533-2	5.071-2	5.529-2	5.950-2
1	53	7.155-4	1.973-4	8.952-5	5.061-5	3.239-5	2.245-5	1.645-5
1	54	1.193-3	3.305-4	1.511-4	8.643-5	5.615-5	3.963-5	2.967-5
1	55	1.667-3	4.597-4	2.086-4	1.179-4	7.546-5	5.229-5	3.833-5
1	56	2.259-2	3.019-2	3.328-2	3.491-2	3.590-2	3.657-2	3.702-2
1	57	3.191-4	6.620-5	2.659-5	1.410-5	8.701-6	5.896-6	4.257-6
1	58	4.472-4	9.363-5	3.828-5	2.085-5	1.330-5	9.387-6	7.101-6
1	59	5.734-4	1.189-4	4.774-5	2.533-5	1.562-5	1.059-5	7.643-6
1	60	7.039-3	8.601-3	9.011-3	9.177-3	9.265-3	9.323-3	9.370-3
1	61	3.291-6	9.160-7	4.092-7	2.283-7	1.447-7	9.946-8	7.254-8
1	62	2.009-5	1.559-5	1.624-5	1.743-5	1.860-5	1.965-5	2.064-5
1	63	1.612-5	4.526-6	2.029-6	1.134-6	7.198-7	4.955-7	3.618-7
1	64	1.437-4	1.640-4	1.868-4	2.062-4	2.225-4	2.363-4	2.487-4
1	65	2.305-5	1.064-5	7.057-6	5.311-6	4.259-6	3.551-6	3.039-6
1	66	2.114-5	8.895-6	5.593-6	4.080-6	3.209-6	2.640-6	2.238-6
1	67	3.157-5	1.138-5	6.698-6	4.922-6	4.062-6	3.573-6	3.271-6
1	68	4.064-5	1.227-5	5.681-6	3.215-6	2.051-6	1.414-6	1.032-6
1	69	2.131-5	6.721-6	3.437-6	2.170-6	1.538-6	1.171-6	9.333-7
1	70	6.768-6	4.381-6	4.084-6	4.052-6	4.074-6	4.108-6	4.141-6
1	71	1.644-5	4.418-6	1.942-6	1.072-6	6.746-7	4.634-7	3.363-7
1	72	1.916-5	6.966-6	4.749-6	4.005-6	3.657-6	3.454-6	3.324-6
1	73	3.402-5	1.220-5	7.824-6	6.030-6	5.020-6	4.350-6	3.863-6
1	74	4.131-5	1.177-5	6.655-6	4.987-6	4.262-6	3.892-6	3.683-6
1	75	4.041-5	1.988-5	1.492-5	1.245-5	1.084-5	9.658-6	8.739-6
1	76	1.185-4	1.234-4	1.223-4	1.196-4	1.167-4	1.141-4	1.117-4
1	77	5.048-5	1.179-5	5.015-6	2.752-6	1.737-6	1.196-6	8.749-7
1	78	6.758-5	8.629-5	1.020-4	1.144-4	1.247-4	1.335-4	1.412-4
1	79	2.511-5	7.313-6	4.018-6	2.817-6	2.213-6	1.846-6	1.598-6
1	80	1.226-5	7.371-6	5.516-6	4.402-6	3.653-6	3.117-6	2.717-6
1	81	3.206-6	6.064-7	2.584-7	1.492-7	1.003-7	7.370-8	5.740-8
1	82	1.084-5	1.346-5	1.516-5	1.622-5	1.691-5	1.738-5	1.773-5
1	83	9.779-6	7.992-6	8.248-6	8.531-6	8.752-6	8.923-6	9.058-6
1	84	1.521-5	3.767-6	2.166-6	1.740-6	1.588-6	1.525-6	1.498-6
1	85	4.825-5	1.223-5	5.396-6	3.040-6	1.964-6	1.385-6	1.038-6
1	86	3.925-5	1.623-5	1.289-5	1.236-5	1.253-5	1.291-5	1.336-5
1	87	1.247-5	3.170-6	1.382-6	7.625-7	4.802-7	3.291-7	2.394-7
1	88	7.156-6	3.137-6	2.168-6	1.672-6	1.362-6	1.148-6	9.925-7
1	89	8.816-6	5.361-6	5.167-6	5.218-6	5.295-6	5.367-6	5.429-6
1	90	9.487-6	1.901-6	8.236-7	4.637-7	2.980-7	2.076-7	1.528-7
1	91	8.631-6	2.003-6	9.824-7	6.338-7	4.655-7	3.675-7	3.037-7
1	92	2.831-5	3.422-5	3.858-5	4.132-5	4.309-5	4.429-5	4.516-5
1	93	4.208-5	4.565-5	4.894-5	5.115-5	5.270-5	5.384-5	5.472-5
1	94	3.797-6	6.927-7	2.597-7	1.317-7	7.876-8	5.216-8	3.701-8
1	95	2.085-4	2.169-4	2.255-4	2.315-4	2.359-4	2.394-4	2.421-4
1	96	9.353-5	1.296-4	1.483-4	1.594-4	1.665-4	1.712-4	1.746-4
1	97	1.887-4	1.828-4	1.831-4	1.849-4	1.868-4	1.887-4	1.905-4
1	98	1.837-3	2.641-3	3.166-3	3.567-3	3.894-3	4.171-3	4.414-3

**Table 6.** Comparisons of effective collision strengths for transitions among the lowest 10 levels of Al X.  $a \pm b \equiv a \times 10^{\pm b}$ .

Transition		RM (log $T_e$ , K)			DARC (log $T_e$ , K)		
I	J	5.90	6.10	6.30	5.90	6.10	6.30
1	2	7.824-3	6.631-3	5.524-3	1.161-2	1.076-2	9.407-3
1	3	2.347-2	1.989-2	1.657-2	3.528-2	3.275-2	2.870-2
1	4	3.912-2	3.316-2	2.762-2	5.881-2	5.444-2	4.753-2
1	5	1.296-0	1.368-0	1.459-0	1.280-0	1.346-0	1.433-0
1	6	2.038-4	1.807-4	1.552-4	6.151-4	6.846-4	6.534-4
1	7	6.113-4	5.420-4	4.657-4	1.744-3	1.930-3	1.834-3
1	8	1.019-3	9.033-4	7.761-4	2.827-3	3.075-3	2.902-3
1	9	1.281-2	1.249-2	1.220-2	1.711-2	1.736-2	1.687-2
1	10	4.581-3	4.495-3	4.383-3	7.199-3	7.312-3	7.000-3
2	3	1.467-1	1.142-1	8.695-2	1.504-1	1.258-1	1.023-1
2	4	1.316-1	1.009-1	7.795-2	1.139-1	9.819-2	8.375-2
2	5	1.749-2	1.472-2	1.231-2	3.116-2	2.919-2	2.533-2
2	6	4.106-3	3.683-3	3.211-3	5.641-3	5.463-3	4.910-3
2	7	6.600-1	6.922-1	7.328-1	6.409-1	6.727-1	7.153-1
2	8	5.527-3	4.973-3	4.356-3	1.148-2	1.163-2	1.061-2
2	9	9.489-3	8.527-3	7.446-3	1.695-2	1.700-2	1.534-2
2	10	1.139-3	1.034-3	9.112-4	2.704-3	2.638-3	2.307-3
3	4	4.821-1	3.721-1	2.844-1	5.072-1	4.196-1	3.430-1
3	5	5.247-2	4.417-2	3.693-2	9.302-2	8.719-2	7.566-2
3	6	6.561-1	6.892-1	7.307-1	6.438-1	6.755-1	7.177-1
3	7	5.150-1	5.408-1	5.734-1	5.057-1	5.292-1	5.588-1
3	8	8.488-1	8.973-1	9.582-1	8.240-1	8.643-1	9.153-1
3	9	2.847-2	2.558-2	2.234-2	5.341-2	5.340-2	4.812-2
3	10	3.417-3	3.102-3	2.734-3	8.667-3	8.480-3	7.434-3
4	5	8.744-2	7.361-2	6.156-2	1.553-1	1.452-1	1.258-1
4	6	5.508-3	4.959-3	4.347-3	9.998-3	1.008-2	9.185-3
4	7	8.499-1	8.984-1	9.590-1	8.273-1	8.675-1	9.186-1
4	8	2.517-0	2.642-0	2.799-0	2.437-0	2.556-0	2.712-0
4	9	4.744-2	4.263-2	3.723-2	1.039-1	1.037-1	9.444-2
4	10	5.694-3	5.170-3	4.556-3	1.587-2	1.547-2	1.351-2
5	6	7.206-3	6.169-3	5.188-3	1.264-2	1.193-2	1.057-2
5	7	2.162-2	1.851-2	1.556-2	3.682-2	3.439-2	3.002-2
5	8	3.603-2	3.084-2	2.594-2	7.226-2	6.812-2	6.101-2
5	9	3.629-0	3.816-0	4.049-0	3.517-0	3.686-0	3.913-0
5	10	1.161-0	1.225-0	1.305-0	1.143-0	1.204-0	1.284-0
6	7	7.308-2	6.478-2	5.610-2	1.016-1	9.890-2	8.872-2
6	8	4.909-2	4.674-2	4.474-2	6.447-2	6.499-2	6.194-2
6	9	3.784-2	3.390-2	2.950-2	4.965-2	4.779-2	4.244-2
6	10	4.239-3	3.724-3	3.158-3	1.008-2	9.699-3	8.374-3
7	8	2.009-1	1.865-1	1.731-1	2.703-1	2.677-1	2.480-1
7	9	1.135-1	1.017-1	8.850-2	1.553-1	1.498-1	1.332-1
7	10	1.272-2	1.117-2	9.473-3	3.065-2	2.926-2	2.514-2
8	9	1.892-1	1.695-1	1.475-1	2.696-1	2.592-1	2.306-1
8	10	2.119-2	1.862-2	1.579-2	5.313-2	5.059-2	4.336-2
9	10	9.438-2	9.645-2	9.929-2	1.141-1	1.172-1	1.181-1

RM: Earlier interpolated results of Keenan et al. (1986)

DARC: Present results from the DARC code



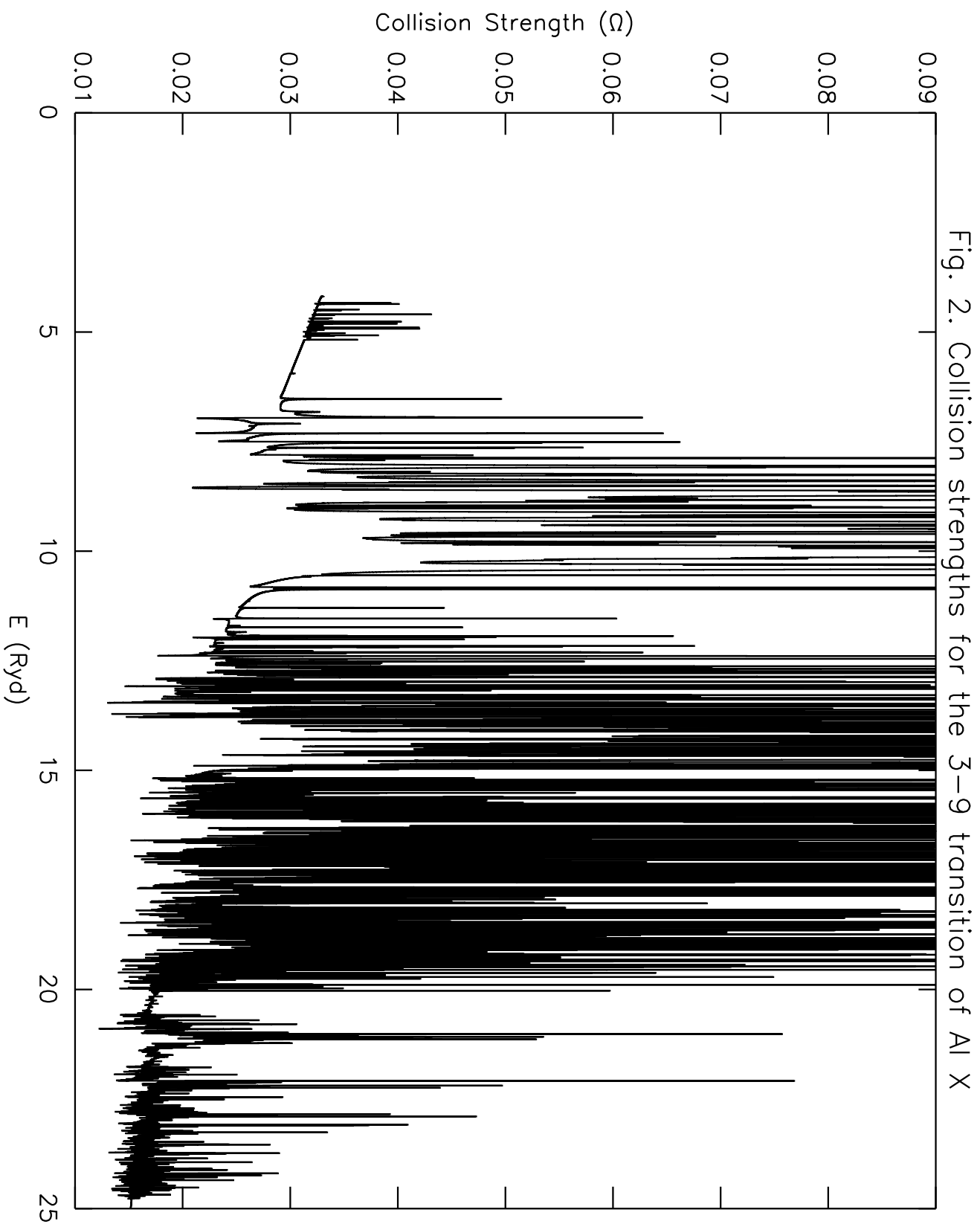


Fig. 2. Collision strengths for the 3–9 transition of Al X